International Journal of Pharmaceutics 556 (2019) 172–180

Contents lists available at ScienceDirect

International Journal of Pharmaceutics

journal homepage: www.elsevier.com/locate/ijpharm

P-glycoprotein (MDR1/ABCB1) and Breast Cancer Resistance Protein (BCRP/ABCG2) limit brain accumulation of the FLT3 inhibitor quizartinib in mice

Jing Wang[a], Changpei Gan[a], Irene A. Retmana[b], Rolf W. Sparidans[b], Wenlong Li[a], Maria C. Lebre[a], Jos H. Beijnen[a,b,c], Alfred H. Schinkel[a,*]

[a] The Netherlands Cancer Institute, Division of Pharmacology, Plesmanlaan 121, 1066 CX Amsterdam, The Netherlands
[b] Utrecht University, Faculty of Science, Department of Pharmaceutical Sciences, Division of Pharmacoepidemiology & Clinical Pharmacology, Universiteitsweg 99, 3584 CG Utrecht, The Netherlands
[c] The Netherlands Cancer Institute/Slotervaart Hospital, Department of Pharmacy & Pharmacology, Plesmanlaan 121, 1066 CX Amsterdam, The Netherlands

ARTICLE INFO

Keywords:
ABCB1
ABCG2
CYP3A enzymes
Quizartinib
Brain penetration
FLT3

ABSTRACT

Quizartinib, a second-generation FLT3 inhibitor, is in clinical development for the treatment of acute myeloid leukemia. We studied its pharmacokinetic interactions with the multidrug efflux transporters ABCB1 and ABCG2 and the multidrug metabolizing enzyme CYP3A, using *in vitro* transport assays and knockout and transgenic mouse models. Quizartinib was transported by human ABCB1 *in vitro*, and by mouse (m)Abcb1 and mAbcg2 *in vivo*. Upon oral administration, the brain accumulation of quizartinib was 6-fold decreased by mAbcb1 and 2-fold by mAbcg2 (together: 12-fold). Unexpectedly, the absence of mAbcb1 resulted in a ~2-fold lower plasma exposure in *Abcb1a/1b*$^{-/-}$ and *Abcb1a/1b;Abcg2*$^{-/-}$ mice, suggesting that loss of mAbcb1 causes compensatory alterations in alternative quizartinib elimination or uptake systems. mAbcb1 and mAbcg2 themselves did not appear to restrict quizartinib oral availability. Oral and intravenous pharmacokinetics of quizartinib were not substantially altered between wild-type, Cyp3a knockout and CYP3A4-humanized mice. All three strains showed relatively high (33–51%) oral bioavailability. If this also applies in humans, this would suggest a limited risk of CYP3A-related inter-individual variation in exposure for this drug. Our results provide a possible rationale for using pharmacological ABCB1/ABCG2 inhibitors together with quizartinib when treating malignant lesions situated in part or in whole behind the blood-brain barrier.

1. Introduction

Acute myeloid leukemia (AML) accounts for 34% of all leukemia cases (Siegel et al., 2017). In 2017, 21,380 new cases were diagnosed, and more than 10,000 patients died from AML in the United States alone (Siegel et al., 2017). Different therapies have been used in treating AML, but despite initial remissions, relapses are frequent, with an overall cure rate of only 30–40% (Rowe and Tallman, 2010).

FMS-like tyrosine kinase 3 (FLT3) is a class III receptor tyrosine kinase (RTK) highly expressed in human hematopoietic stem and progenitor cells (Meshinchi and Appelbaum, 2009). Activating mutations in FLT3 have been identified in up to 30% of AML patients (Gilliland and Griffin, 2002; Levis and Small, 2005). The commonest gain-of-function mutation in FLT3 is internal tandem duplications (ITDs), present in approximately 30% of cytogenetically normal AML (Meshinchi and Appelbaum, 2009; Döhner et al., 2015). FLT3-ITD mutations are associated with increased relapse rates and reduced overall survival when treated with standard therapy (Thiede et al., 2002; Schnittger et al., 2002; Kottaridis et al., 2001), or after allogeneic haematopoietic stem cell transplantation (Fleischmann et al., 2017). These mutations are also negative prognostic factors for the survival of refractory or relapsed AML patients because of their poor response to rescue therapy (Wattad et al., 2017; Schlenk et al., 2017; Chevallier et al., 2011; Wagner et al., 2011).

Tyrosine kinase inhibitors (TKIs) are promising agents in the treatment of FLT3-ITD mutated AML, especially in combination with chemotherapy (Kindler et al., 2010; Benderra et al., 2005). The first-generation FLT3 inhibitors, sunitinib (Fiedler et al., 2015) and sorafenib, have been used in the treatment of AML, but treatment with sorafenib did not result in significant improvement in the median event-

* Corresponding author.
E-mail address: a.schinkel@nki.nl (A.H. Schinkel).

https://doi.org/10.1016/j.ijpharm.2018.12.014
Received 21 September 2018; Received in revised form 27 November 2018; Accepted 3 December 2018
Available online 12 December 2018

free survival or overall survival. The risk for bleeding events, fever, and hand-foot syndrome was significantly higher in the sorafenib arm of the study (Serve et al., 2013; Röllig et al., 2014). Interestingly, sorafenib combined with conventional chemotherapy achieved complete remission in a study with FLT3-ITD–positive AML (Baker et al., 2013). However, conventional cancer chemotherapy may cause a range of side effects which can adversely affect patients' health and quality of life.

Quizartinib (AC220) is a second-generation FLT3 inhibitor, with better pharmaceutical and pharmacokinetic properties, and much greater target specificity than sunitinib and sorafenib. *In vitro*, quizartinib is a potent inhibitor of both wild-type FLT3 and mutant FLT3-ITD. The inhibition of mutant-FLT3 isoforms results in inhibition of cellular proliferation and induction of apoptosis (Zarrinkar et al., 2009; Chao et al., 2009; Kampa-Schittenhelm et al., 2013). In phase 1 trials, quizartinib showed efficacy in patients with relapsed or refractory AML with wild-type FLT3 as well as FLT3-ITD (Cortes et al., 2013), and it appears to be a safe single-dose agent with no serious adverse events (Sanga et al., 2017). Quizartinib is currently evaluated in clinical (phase 2/3) trials in combination with omacetaxine mepesuccinate or chemotherapy in newly diagnosed or relapsed/refractory AML carrying FLT3-ITD mutations (www.clinicaltrials.gov: NCT03135054, NCT02668653). Recent preclinical studies show that quizartinib may also be used to transiently induce quiescence in multipotent hematopoietic progenitor cells, thus circumventing myelosuppression by coadministered cytotoxic chemotherapeutics like 5-FU and gemcitabine (Taylor et al., 2017). If this turns out to also apply in humans, this could present a major advance in limiting myelosuppression, which is often dose-limiting in cytotoxic cancer chemotherapy.

ABCB1 (P-glycoprotein/MDR1) and ABCG2 (Breast Cancer Resistance Protein/BCRP) are multispecific drug efflux transporters localized at apical membranes of liver, kidney and intestine, where they pump their substrates into bile, urine, and feces, respectively. They also occur at pharmacological sanctuary site barriers such as the blood-brain barrier (BBB) and blood-testis barrier, where they pump their substrates back into blood. As a consequence, only small amounts of drug can accumulate in, for instance, the brain, which can compromise treatment of (micro-)metastases that are present behind a functionally intact BBB (Borst and Elferink, 2002; Schinkel and Jonker, 2003; Vlaming et al., 2009). The FLT3 inhibitors sorafenib and sunitinib are good transport substrates of human (h) ABCB1 and ABCG2 and mouse (m)Abcg2, and their brain accumulation is effectively restricted by both mAbcb1 and mAbcg2 activity *in vivo* (Tang et al., 2013; Tang et al., 2012a; Lagas et al., 2010; Tang et al., 2012b). Current data suggest that quizartinib acts as an inhibitor of ABCB1 and ABCG2 *in vitro* (Bhullar et al., 2013) and of ABCG2 also *in vivo* (Li et al., 2017), but there are no indications that it can be transported by ABCB1 or ABCG2. In fact, K562 cell lines overexpressing ABCB1 or ABCG2 even showed increased sensitivity to this drug ("collateral sensitivity", see Pluchino et al., 2012), arguing against efficient export of quizartinib by ABCB1 and ABCG2 in this cell line (Bhullar et al., 2013).

Cytochrome P450-3A (CYP3A) is an abundant multispecific drug-metabolizing enzyme highly expressed in human liver and small intestine, and it plays a significant role in the metabolism of approximately half of the drugs in current clinical use (Guengerich, 1995; Zanger and Schwab, 2013). As CYP3A can display a high degree of inter- and intra-individual activity, it is a major player in variable drug exposure (van Waterschoot et al., 2009; van Hoppe et al., 2017). Quizartinib is quite extensively metabolized in humans, and it may be an *in vitro* CYP3A substrate (Cortes et al., 2013; Sanga et al., 2017).

Plasma pharmacokinetics as well as tissue and tumor distribution can have a major impact on the therapeutic efficacy of a drug. In this study we therefore aimed to investigate whether quizartinib is transported by ABCB1 and ABCG2 *in vitro*, and to establish the *in vivo* effects of these transporters and of CYP3A on oral availability and tissue distribution of quizartinib in wild-type and knockout mouse strains.

2. Material and methods

2.1. Chemicals

Quizartinib (98.5%, M_w = 560.7 g/mol) and zosuquidar were obtained from Sequoia Research Products (Pangbourne, UK). Ko143 was from Tocris Bioscience (Bristol, UK). Bovine Serum Albumin (BSA) Fraction V was obtained from Roche Diagnostics (Mannheim, Germany). Isoflurane was purchased from Pharmachemie (Haarlem, The Netherlands), heparin (5000 IU ml^{-1}) was from Leo Pharma (Breda, The Netherlands). Chemicals used in the quizartinib assay were described before (Retmana et al., 2017). All other chemicals and reagents were obtained from Sigma-Aldrich (Steinheim, Germany).

2.2. Transport assays

Polarized Madin-Darby Canine Kidney (MDCK-II) cell lines transduced with human (h)ABCB1, hABCG2 and mouse (m)Abcg2 cDNA were used (passage 10–20 after clonal selection) and cultured as described previously (Durmus et al., 2012). We never generated MDCKII cells overexpressing mAbcb1a or mAbcb1b, given the near-complete overlap in substrate specificity with hABCB1. Transepithelial transport assays were performed in triplicate using 12-well microporous polycarbonate membrane filters (3.0-μm pore size, Transwell 3402, Corning., Lowell, MA) as previously described (Durmus et al., 2012). In short, cells were seeded on the same day and at the same density (5×10^5 cells per well), and allowed to grow an intact monolayer in 3 days, which was monitored with transepithelial electrical resistance (TEER) measurements. 5 μM each of quizartinib, zosuquidar (ABCB1 inhibitor) and/or Ko143 (ABCG2/Abcg2 inhibitor) were used during the transport experiments. On the third day, if applicable, cells were pre-incubated with one or more of the inhibitors for 1 h in both compartments. The transport phase was initiated (t = 0) by replacing the medium in both compartments with fresh Dulbecco's Modified Eagle's medium (DMEM medium) including 10% fetal bovine serum (FBS) and quizartinib at 5 μM, as well as the appropriate inhibitor(s). Cells were kept at 37 °C in 5% (v/v) CO_2 during the experiment, and at 1, 2, 4 and 8 h, 50 μl samples were taken from the acceptor compartment, and stored at −30 °C until LC-MS/MS analysis. The amount of transported drug was calculated after correction for volume loss due to sampling at each time point. Active transport was expressed using the transport ratio (r), which is defined as the amount of apically directed drug transport divided by basolaterally directed drug translocation at a defined time point.

2.3. Animals

Mice (*Mus musculus*) were bred in the Netherlands Cancer Institute and housed and handled according to institutional guidelines complying with Dutch and EU legislation. All experiments were reviewed and approved by the Institutional Animal Care and Use Committee (IACUC). Animals used were female WT, *Abcb1a/1b*$^{-/-}$ (Schinkel et al., 1997), *Abcg2*$^{-/-}$ (Jonker et al., 2002), *Abcb1a/1b;Abcg2*$^{-/-}$ (Jonker et al., 2005) and *Cyp3a*$^{-/-}$ (van Herwaarden et al., 2007) mice of a > 99% FVB/N strain background. Homozygous CYP3A4 humanized transgenic mice (Cyp3aXAV) were generated by cross-breeding of transgenic mice with stable human CYP3A4 expression in liver or intestine, respectively, in a *Cyp3a*$^{-/-}$ background (van Herwaarden et al., 2007). All the mice used were between 9 and 14 weeks of age, and generally between 23 and 35 g of body weight. Animals were kept in a temperature-controlled environment with a 12 h light/12 h dark cycle and received a standard diet (Transbreed, SDS Diets, Technilab-BMI) and acidified water *ad libitum*. Depending on the type of experiment, between 4 and 6 mice were tested in each experimental group.

2.4. Drug solutions

Quizartinib stock solution was in dimethylsulfoxide (DMSO) at a concentration of 33.3 mg/ml stored at −30 °C, and subsequently diluted with 50 mM sodium acetate buffer (pH 4.4) to yield a working concentration of 1 mg/ml. The final DMSO concentration in the formulation was 3%. All working solutions were prepared freshly on the day of the experiment.

2.5. Plasma and tissue pharmacokinetics of quizartinib

For the oral experiment, quizartinib (10 mg/kg) was administered to the mice by oral gavage using a blunt-ended needle. To minimize variation in absorption, mice were fasted for about 2 h before quizartinib was administered (n = 4–6). For the intravenous experiment, quizartinib (5 mg/kg) was injected into the tail vein (n = 4–6). For the 24 or 8 h experiments, 50 µl blood samples were collected from the tail vein at 0.5, 1, 2, 4 and 8 h or 0.25, 0.5, 1, 2 and 4 h, respectively, using heparin-coated capillaries (Sarstedt, Germany). At 24 or 8 h, mice were anesthetized with isoflurane and blood was collected by cardiac puncture. Immediately thereafter, mice were sacrificed by cervical dislocation, and the brain and a set of other tissues were removed, weighed and rapidly frozen at − 30 °C. Tissues were homogenized on ice in an appropriate volume of 4% (w/v) BSA in water, and stored further at − 30 °C until analysis. Blood samples were centrifuged at 9,000 *g* for 6 min at 4 °C immediately after collection, and the plasma fractions were collected and stored at − 30 °C until analysis.

2.6. LC-MS/MS analysis

Quizartinib concentrations in cell culture medium, plasma and tissue homogenates were analyzed with a previously reported liquid-chromatography tandem mass spectrometric (LC-MS/MS) assay, using a deuterated internal standard (Retmana et al., 2017).

2.7. Statistics and pharmacokinetic calculations

Pharmacokinetic parameters were calculated by the software GraphPad Prism7 (GraphPad Software Inc., La Jolla, CA, USA). The area under the plasma concentration-time curve (AUC) was calculated using the trapezoidal rule with the Microsoft Excel plug in PKsolver (Zhang et al., 2010), without extrapolating to infinity. Ordinary one-way analysis of variance (ANOVA) was used to determine significance of differences between groups, after which post-hoc tests with Tukey correction were performed for comparison between individual groups. The two-sided unpaired Student's *t* test was used when treatments or differences between two groups were compared. The peak plasma concentration (C_{max}) and the time to reach C_{max} (t_{max}) were estimated from the original data. Relative organ accumulation (P_{organ}) was calculated by dividing organ concentrations (C_{organ}) at either t = 24 h or t = 8 h by the $AUC_{0\text{-}24h}$ or $AUC_{0\text{-}8h}$, respectively. Differences were considered statistically significant when $P < 0.05$. Data are presented as mean ± SD with each experimental group containing 4–6 mice.

3. Results

3.1. Quizartinib is moderately transported by hABCB1 in vitro

We analyzed quizartinib (5 µM) transport across polarized Madin-Darby Canine Kidney (MDCK-II) cell lines stably transduced with human (h)ABCB1, hABCG2, or mouse (m)Abcg2 cDNA. The MDCK-II parental cells did not show significant apically directed transport (Fig. 1A, efflux ratio r = 0.8), and addition of the ABCB1 inhibitor zosuquidar did not change this result (Fig. 1B, r = 0.7). In hABCB1-overexpressing MDCKII cells, we observed clear apically directed transport of quizartinib (Fig. 1C, r = 2.6), which was completely inhibited by co-incubation with zosuquidar (Fig. 1D, r = 0.9). To suppress any possible transport contribution of quizartinib by the endogenous canine ABCB1, subsequent experiments were all done in the presence of zosuquidar (5 µM). In hABCG2-overexpressing MDCK-II cells, no clear net transport of quizartinib was detected, and addition of Ko143 did not alter this profile (r = 0.9 and 0.8, respectively, Fig. 1E and F). In mAbcg2-overexpressing MDCK-II cells, there was a slight apically directed transport of quizartinib r = 1.5 (Fig. 1G), and this could be reduced with the ABCG2 inhibitor Ko143 to an r of 1.2 (Fig. 1H). These data demonstrate that quizartinib at 5 µM is moderately transported by hABCB1, but not noticeably by hABCG2, and perhaps by mAbcg2 *in vitro*, although the latter did not reach statistical significance.

3.2. Roles of Abcb1 and Abcg2 in quizartinib oral availability and tissue distribution

In view of the *in vitro* transport data, we also wanted to assess the *in vivo* impact of Abcb1 and Abcg2 on quizartinib oral availability and tissue distribution. Since quizartinib is given orally to patients at a dose of ~200 mg, we administered this drug to mice by oral gavage into the stomach at a physiologically roughly equivalent dose of 10 mg/kg.

We first performed a 24-hour pilot study in female WT and *Abcb1a/1b;Abcg2*$^{-/-}$ mice. After oral administration, the plasma concentrations were high, with a C_{max} of 1.6–2 µg/ml in both mouse strains, and a t_{max} around 8 h. At t = 24 h, the plasma concentrations in both strains were similar. The combined absence of Abcb1a/1b and Abcg2 resulted in 0.8-fold lower plasma $AUC_{0\text{-}24}$, although this was not statistically significant (Fig. 2A; Supplemental Table 1). We next measured the brain, liver, kidney and spleen concentrations of quizartinib 24 h after oral administration. Although at t = 24 h the plasma concentrations in both strains were similar, the brain concentration in *Abcb1a/1b;Abcg2*$^{-/-}$ mice was markedly (17.8-fold) higher than that in WT mice (Fig. 3A; Supplemental Table 1). The same applied for the brain-to-plasma ratio (12-fold) and the relative brain accumulation (24-fold) (Fig. 3B and C; Supplemental Table 1). In contrast to the brain, we observed no significant differences between the strains in liver concentration, liver-to-plasma ratio (400–500%) and liver accumulation (Fig. 3D–F). Qualitatively similar data were obtained for kidney and spleen concentrations, tissue-to-plasma ratios (150–250% for kidney and 140% for spleen), and tissue accumulations of quizartinib between these strains (Supplemental Fig. 1A–F). The tissue-to-plasma distribution ratios for these organs in WT mice (140–500%) were all far higher than those observed for the WT brain (~10%). These data suggest that quizartinib is kept mostly out of the brain by mAbcb1a/1b and/or mAbcg2, but that these proteins have no substantial effect on relative quizartinib distribution to liver, kidney, and spleen after oral administration.

To better assess the impact on plasma concentration and tissue distribution of quizartinib, as well as the possible single and overlapping pharmacokinetic roles of mAbcb1 and mAbcg2 at the BBB, we performed another oral quizartinib (10 mg/kg) experiment including WT, *Abcb1a/1b;Abcg2*$^{-/-}$, as well as single Abcg2 and Abcb1a/1b knockout mice. We terminated at t = 8 h, i.e. not far from the quizartinib C_{max} and t_{max} in each strain (Fig. 2A and B). As shown in Fig. 2B, the plasma $AUC_{0\text{-}8}$ in the single Abcg2 knockout mice was lower than in WT mice, but this was not statistically significant (0.8-fold, $P > 0.05$). In contrast, the *Abcb1a/1b*$^{-/-}$ and *Abcb1a/1b;Abcg2*$^{-/-}$ mice both showed a significantly lower $AUC_{0\text{-}8}$ than the WT mice (0.56-fold, $P < 0.01$; 0.47-fold, $P < 0.01$, respectively; Table 1). Of note, also in the preceding 24 h experiment the $AUC_{0\text{-}8}$ in *Abcb1a/1b;Abcg2*$^{-/-}$ mice had been significantly reduced compared to WT mice (0.65-fold, $P < 0.05$, Supplemental Table 1), indicating qualitative consistency between these experiments.

We also measured the brain concentrations of quizartinib at 8 h. The single *Abcg2*$^{-/-}$ mice did not display statistically significant changes in

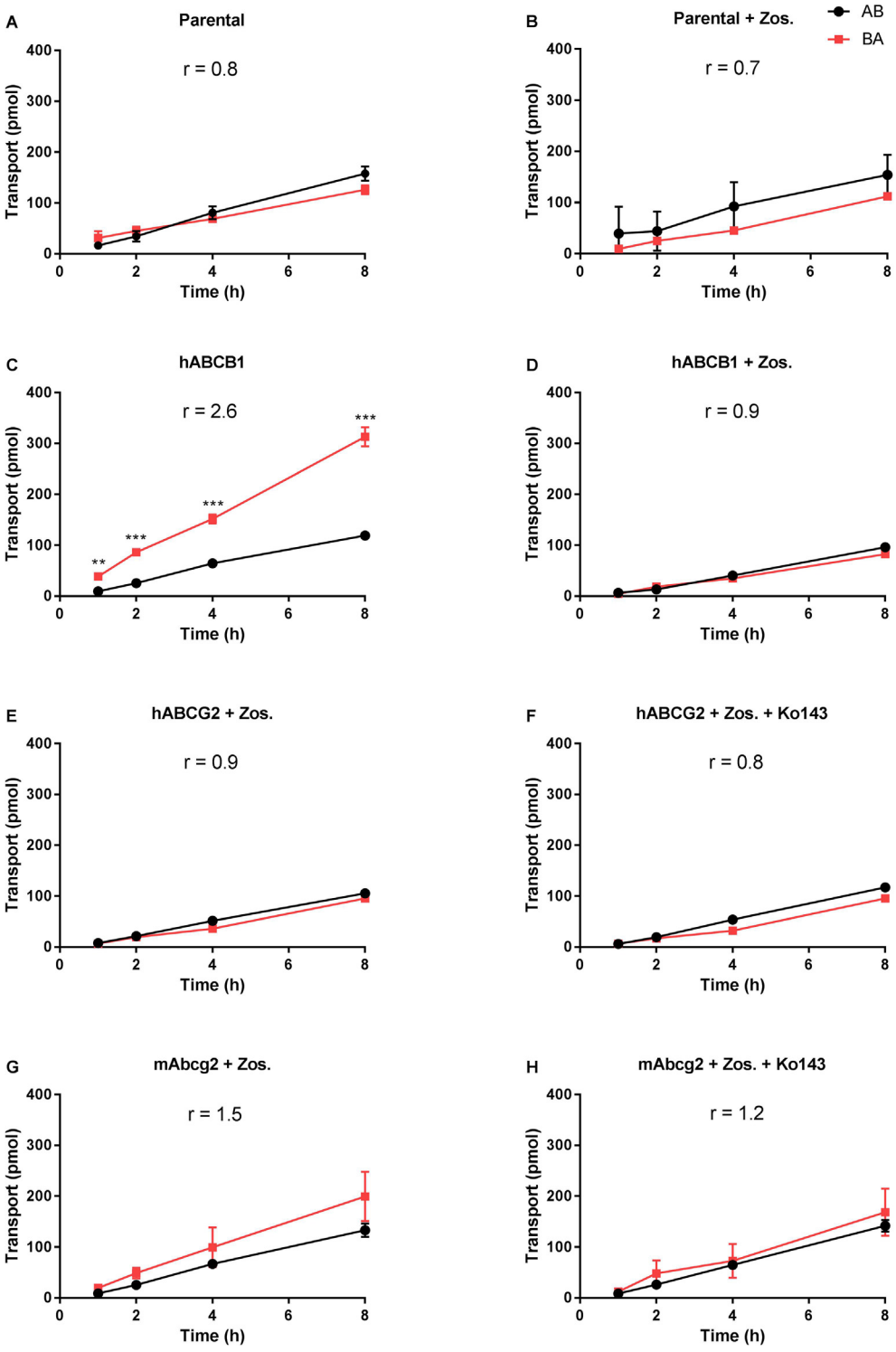

Fig. 1. In vitro transport of quizartinib. Transepithelial transport of quizartinib (5 µM) was assessed in MDCK-II cells either non-transduced (A, B) or transduced with hABCB1 (C, D), hABCG2 (E, F) or mAbcg2 (G, H) cDNA. At t = 0 h, quizartinib was applied to the donor compartment and the concentrations in the acceptor compartment at t = 1, 2, 4 and 8 h were measured and plotted as total amount of transport (pmol) in the graphs (n = 3). B, D–H: Zos. (zosuquidar, 5 µM) and/or Ko143 (5 µM) were applied as indicated to inhibit ABCB1 and hABCG2 or mAbcg2, respectively. r, relative transport ratio. BA (■), translocation from the basolateral to the apical compartment; AB (●), translocation from the apical to the basolateral compartment. Points, mean; bars, SD. *, $P < 0.05$; **, $P < 0.01$; ***, $P < 0.001$ compared to AB.

brain concentrations, brain-to-plasma ratios and brain accumulations compared to WT mice. However, in spite of the significantly lower plasma concentrations in *Abcb1a/1b*$^{-/-}$ and *Abcb1a/1b;Abcg2*$^{-/-}$ mice at 8 h, the quizartinib brain concentrations were greatly increased in these two mouse strains compared to WT mice, and accordingly also the brain-to-plasma ratios (5.6- and 11.8-fold, respectively) and brain accumulations (Fig. 3G–I; Table 1). The observation that the brain-to-plasma ratio was substantially higher in the *Abcb1a/1b;Abcg2*$^{-/-}$ mice than in the *Abcb1a/1b*$^{-/-}$ mice (Fig. 3H) suggests that mAbcg2 also contributes to reducing the brain accumulation of quizartinib. Collectively, these data indicate that the brain penetration of quizartinib was limited by both mAbcb1 and mAbcg2, albeit with a substantially bigger role for mAbcb1. We further analyzed the liver (Fig. 3J–L) as well as the kidney and spleen concentrations (Supplemental Fig. 1G–L) of quizartinib at 8 h after oral administration. Like in the 24 h experiment, we found no substantial effect of mAbcb1 and mAbcg2 on relative quizartinib distribution to these organs after oral administration.

3.3. Limited in vivo role of Cyp3a in quizartinib pharmacokinetics

To investigate the possible impact of mCyp3a and hCYP3A4 on quizartinib pharmacokinetics in mice, we first performed an 8 h oral

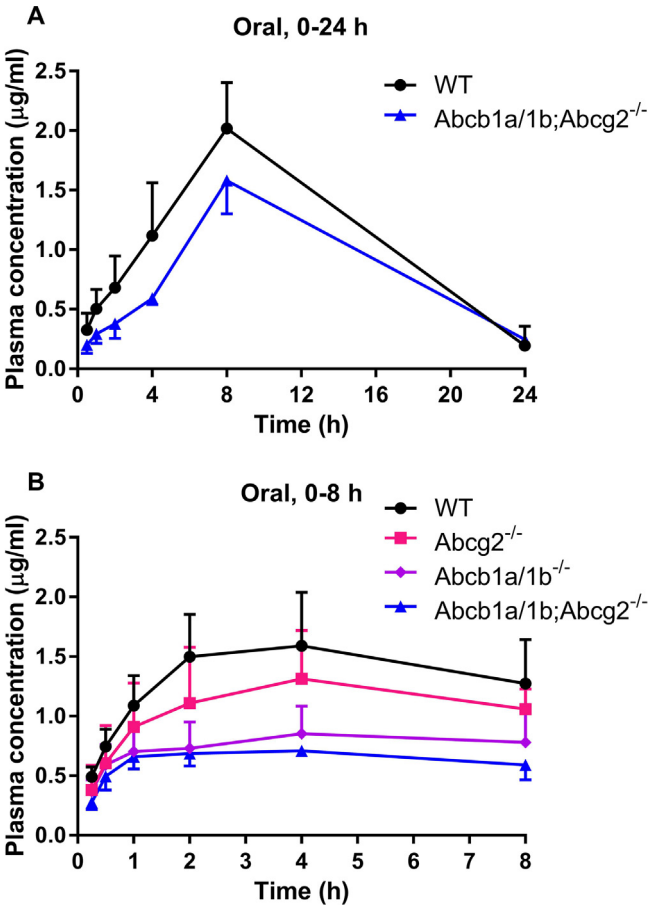

Fig. 2. Plasma concentration–time curves of quizartinib in female WT and *Abcb1a/1b;Abcg2*$^{-/-}$ mice over 24 h (A) or in WT, *Abcg2*$^{-/-}$, *Abcb1a/1b*$^{-/-}$ and *Abcb1a/1b;Abcg2*$^{-/-}$ mice over 8 h (B) after oral administration of 10 mg/kg quizartinib. Data are given as mean ± S.D. (n = 4–6).

study in WT, Cyp3a knockout and Cyp3aXAV mice (Cyp3aXAV mice are humanized transgenic mice with stable human CYP3A4 expression in liver and intestine, in a Cyp3a knockout background). We found no meaningful differences in the plasma exposure of quizartinib over 8 h ($AUC_{0\text{-}8}$) in these three strains. The C_{max} in *Cyp3a*$^{-/-}$ and Cyp3aXAV mice occurred in both around 8 h. At this time point, Cyp3aXAV mice showed, somewhat unexpectedly, significantly higher plasma concentrations than WT and *Cyp3a*$^{-/-}$ mice, $P < 0.001$, $P < 0.05$, respectively (Fig. 4A).

To further investigate the quizartinib pharmacokinetics, we also performed a 24 h oral and intravenous study in female WT, *Cyp3a*$^{-/-}$ and Cyp3aXAV mice, at a dose of 10 mg/kg (oral), and 5 mg/kg (intravenous, with reduced dose to accommodate quizartinib solubility limits). The oral plasma $AUC_{0\text{-}24}$ was not significantly changed between *Cyp3a*$^{-/-}$ and WT mice, but Cyp3aXAV mice did show a significantly higher $AUC_{0\text{-}24}$ than WT and *Cyp3a*$^{-/-}$ mice (1.6-fold; Fig. 4B; Table 2). Upon intravenous administration of quizartinib, the plasma exposure of quizartinib over 24 h ($AUC_{0\text{-}24}$) was slightly but significantly increased in *Cyp3a*$^{-/-}$ and Cyp3aXAV mice compared to WT mice (Supplemental Fig. 2A and B; Table 2). Collectively, the changes in plasma exposure observed between the strains were modest, albeit now and then significant. However, the direction of the changes was rather unexpected: assuming that mouse Cyp3a and human CYP3A4 would each substantially contribute to the metabolism of quizartinib, one would expect an increase in plasma AUC in *Cyp3a*$^{-/-}$ mice, and a subsequent decrease in Cyp3aXAV mice. Clearly that was not observed here. However, the modest shifts observed, and their unexpected direction suggest that Cyp3a itself is not a major determinant of quizartinib pharmacokinetics in mice.

When we measured the brain, liver, kidney, and spleen concentrations of quizartinib at 8 and 24 h after oral administration, we found no meaningful differences in tissue-to-plasma ratios after 8 h (Supplemental Fig. 3) or 24 h (Supplemental Fig. 4). These data suggest that mCyp3a and hCYP3A4 do not to have a substantial impact on quizartinib distribution to brain, liver, kidney, or spleen after oral administration. Liver and kidney appeared to equilibrate fairly efficiently with plasma levels of quizartinib also after intravenous administration, with very similar tissue-to-plasma ratios between the different strains after 24 h (Supplemental Fig. 5). Tissue-to-plasma distribution ratios were also similar to those seen after oral quizartinib administration, with ~600% and ~250% for liver and kidney, respectively.

Because quizartinib was orally and intravenously administered to mice at different dosages (10 or 5 mg/kg), we used the normalized oral and i.v. $AUC_{0\text{-}24}$ to estimate the oral bioavailability of quizartinib in the different CYP3A-modified mouse strains (Fig. 5). The data suggest that the oral bioavailability of quizartinib was relatively high (33–51%) over 24 h in all three tested strains. Although the changes between the strains were very modest, the observed trends in the shifts were again in contrast with the assumption that mouse Cyp3a and human CYP3A4 limit the oral bioavailability of quizartinib, with ablation of mouse Cyp3a resulting in a small decrease in apparent bioavailability, and subsequent overexpression of human CYP3A4 resulting in a modest increase in apparent bioavailability. Perhaps (modest) secondary changes in expression of putative other detoxifying systems affecting quizartinib resulting from the engineered genetic modifications may have caused these minor shifts.

4. Discussion

We found that quizartinib is moderately transported by hABCB1 and possibly slightly by mAbcg2, but not noticeably by hABCG2 *in vitro*. Consistent with a moderately transported Abcb1 substrate and a slightly transported Abcg2 substrate, the brain penetration of quizartinib in mice was clearly limited by the combined function of mAbcb1 and mAbcg2 (11.8-fold), and by single mAbcb1 activity as well (5.6-fold). Thus, both mAbcb1 and mAbcg2 can restrict brain accumulation of quizartinib in mice. mAbcb1 could fully compensate for the loss of mAbcg2 at the BBB, as *Abcg2*$^{-/-}$ and WT mice had similar quizartinib brain penetration levels. In contrast, mAbcg2 can only very partly take over the function of mAbcb1 at the BBB when mAbcb1 is absent. These data confirm that quizartinib is not only transported by mAbcb1 *in vivo*, but also by mAbcg2.

Somewhat unexpectedly, upon oral administration to mice, the absence of mAbcb1 resulted in a significantly, about 2-fold lower plasma $AUC_{0\text{-}8}$ in *Abcb1a/1b*$^{-/-}$ and *Abcb1a/1b;Abcg2*$^{-/-}$, but not *Abcg2*$^{-/-}$ mice. This suggests that loss of mouse Abcb1 (but not Abcg2) may perhaps secondarily cause compensatory upregulation of an alternative quizartinib elimination system or decrease of a quizartinib uptake system, resulting in decreased overall quizartinib exposure. We have previously observed compensatory upregulation of functionally related detoxification systems for a drug due to inactivation of other detoxification systems in mice. For instance, knockout of mouse Cyp3a genes resulted in compensatory upregulation of mouse Cyp2c genes, which compensated for an expected reduction in midazolam metabolism (van Waterschoot et al., 2008). Follow-up studies indicated that this was most likely due to food-derived xenobiotic compounds activating the nuclear receptors PXR and CAR, which subsequently activated expression of the Cyp2c genes (van Waterschoot et al., 2009). Normally these xenobiotic inducing compounds would probably be rapidly degraded by Cyp3a activity. However this may be, it appears unlikely that Abcb1 and Abcg2 themselves in the intestine and/or liver can markedly reduce overall systemic uptake of quizartinib after oral administration, as this should have resulted in increased plasma levels upon ablation of these proteins. The nature of putative compensatorily

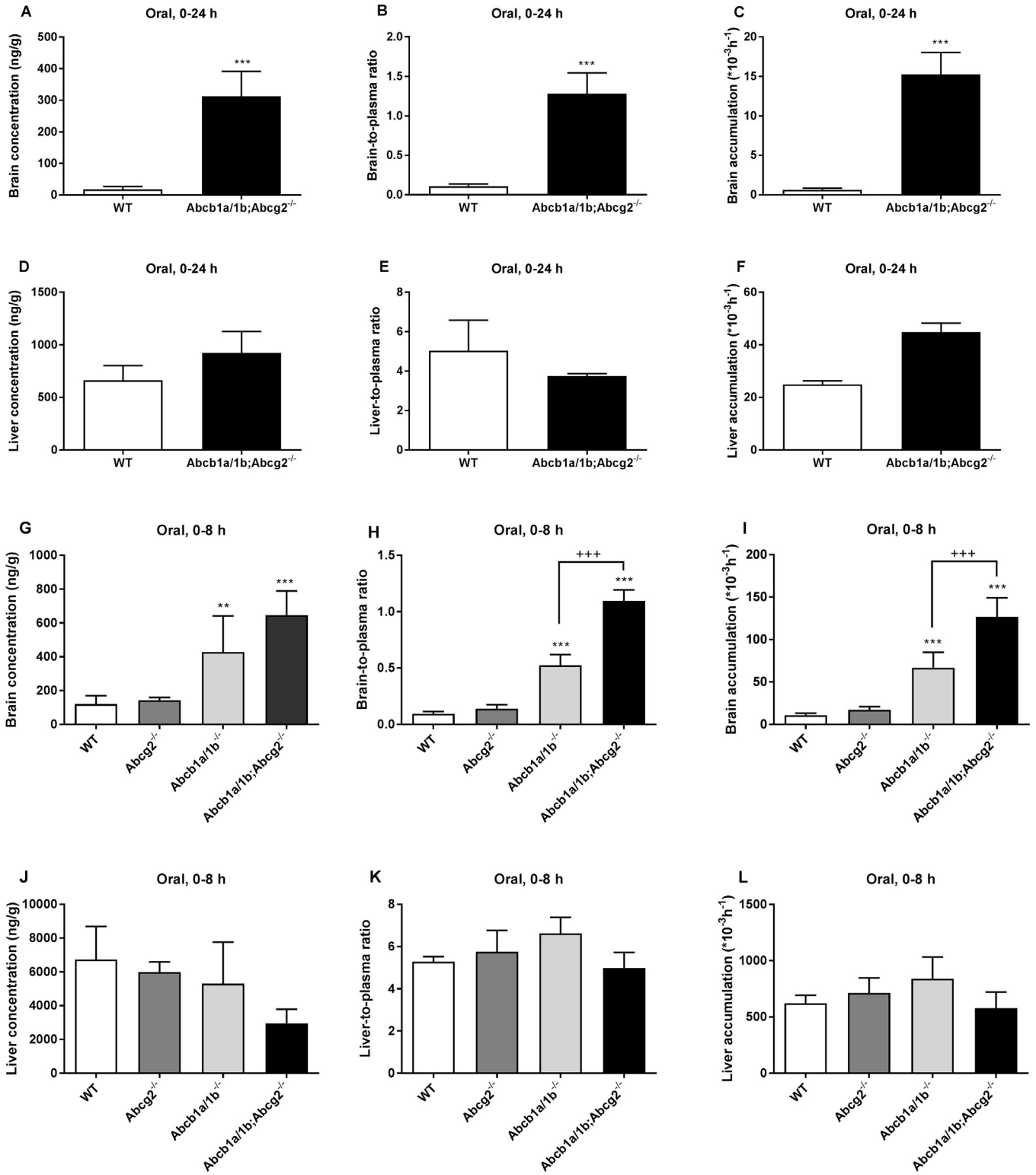

Fig. 3. A-F: brain and liver concentration (A, D), tissue-to-plasma ratio (B, E) and tissue accumulation (C, F) of quizartinib in female WT and *Abcb1a/1b;Abcg2*$^{-/-}$ mice at 24 h after oral administration of quizartinib at 10 mg/kg (n = 4–6). G-L: brain and liver concentration (G, J), tissue-to-plasma ratio (H, K) and tissue accumulation (I, L) of quizartinib in female WT, *Abcg2*$^{-/-}$, *Abcb1a/1b*$^{-/-}$ and *Abcb1a/1b;Abcg2*$^{-/-}$ mice 8 h after oral administration of quizartinib at 10 mg/kg (n = 4–6). *, $P < 0.05$; **, $P < 0.01$; ***, $P < 0.001$ compared to WT mice.

altered detoxification system(s) responsible for the decreased systemic exposure to quizartinib in the Abcb1-deficient strains will be an interesting question for follow-up studies.

Our demonstration that quizartinib is clearly transported by hABCB1 *in vitro* and by mAbcb1 and mAbcg2 in the BBB of mice contrasts with a previous report suggesting that hABCB1 and hABCG2 overexpression caused no resistance, but instead substantial collateral sensitivity (8- and 5-fold, respectively) to quizartinib in the K562 myelogenous leukemia cell line (Bhullar et al., 2013). It also contrasts with a report that hABCG2 does not confer significant resistance to

Table 1
Plasma pharmacokinetic parameters and brain concentration 8 h after oral administration of 10 mg/kg quizartinib to female WT, *Abcg2*$^{-/-}$, *Abcb1a/1b*$^{-/-}$, *Abcb1a/1b;Abcg2*$^{-/-}$, *Cyp3a*$^{-/-}$ and Cyp3aXAV mice.

Parameter	Genotype					
	WT	*Abcg2*$^{-/-}$	*Abcb1a/1b*$^{-/-}$	*Abcb1a/1b;Abcg2*$^{-/-}$	*Cyp3a*$^{-/-}$	Cyp3aXAV
Plasma AUC_{0-8} (h*μg/ml)	10.8 ± 2.5	8.7 ± 2.3	6.1 ± 1.7 **	5.12 ± 0.4 **	12.2 ± 1.8	13.9 ± 2.4
Fold change AUC_{0-8}	1	0.81	0.56	0.47	1.13	1.29
C_{max} (μg/ml)	1.7 ± 0.4	1.4 ± 0.4	0.9 ± 0.3	0.8 ± 0.1	1.9 ± 0.2	2.5 ± 0.3
t_{max} (h)	2–4	2–8	2–8	2–8	2–8	4–8
C_{brain} (ng/g)	121 ± 49	143 ± 16	428 ± 214 **	647 ± 142 ***	167 ± 24	244 ± 33
Fold change C_{brain}	1	1.2	3.5	5.4	1.4	2.0
Brain-to-plasma ratio	0.09 ± 0.02	0.14 ± 0.04	0.52 ± 0.10 **	1.10 ± 0.10 ***	0.10 ± 0.01	0.10 ± 0.00
Fold change ratio	1	1.5	5.6	11.8	1.0	1.1
P_{brain} (*10^{-3}h^{-1})	10.8 ± 2.3	17.1 ± 3.8	66.8 ± 18.1 **	126.7 ± 22.4 ***	13.8 ± 1.3	17.8 ± 2.9
Fold change P_{brain}	1	1.6	6.2	11.7	1.3	1.7

Data are given as mean ± S.D. (n = 4–6). C_{max}, maximum concentration in plasma; t_{max}, time point (h) of maximum plasma concentration (range for individual mice); C_{brain}, brain concentration; P_{brain}, brain accumulation. *, $P < 0.05$; **, $P < 0.01$; ***, $P < 0.001$ compared to WT mice.

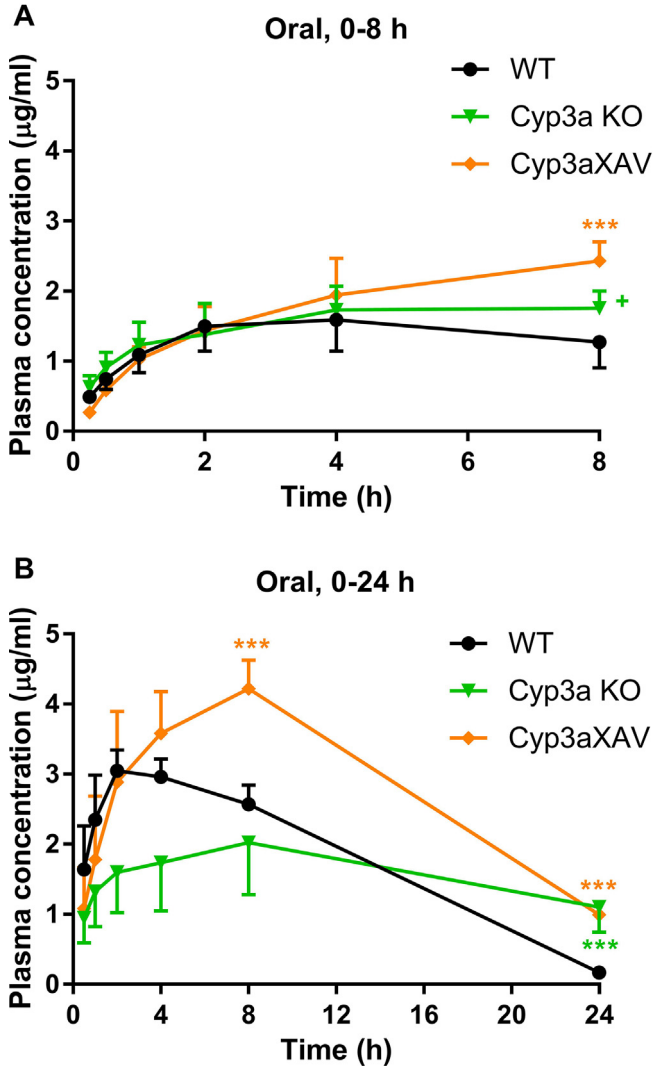

Fig. 4. Plasma concentration–time curves of quizartinib in female WT, Cyp3a KO and Cyp3aXAV mice over 8 h (A) or 24 h (B) after oral administration of 10 mg/kg quizartinib. Data are given as mean ± S.D. (n = 4–6). *, $P < 0.05$; **, $P < 0.01$; ***, $P < 0.001$ compared to WT mice. +, $P < 0.05$ compared to Cyp3aXAV mice.

quizartinib when overexpressed in H460 or HEK293 cell lines (Li et al., 2017). It may be that hABCG2 is only a poor transporter of quizartinib compared to the already modest transporter mAbcg2, and perhaps

Table 2
Plasma pharmacokinetic parameters over 24 h after oral (10 mg/kg) or intravenous (5 mg/kg) administration of quizartinib to female WT, *Cyp3a*$^{-/-}$ and Cyp3aXAV mice.

Parameter	Dosing	Genotype		
		WT	*Cyp3a*$^{-/-}$	Cyp3aXAV
Plasma AUC_{0-24} (h*μg/ml)	Oral, 10 mg/kg	43.0 ± 4.1	38.1 ± 8.5 +++	67.1 ± 5.5 ***
Fold change AUC_{0-24}		1	0.9	1.6
C_{max} (μg/ml)		3.1 ± 0.3	2.1 ± 0.7	4.2 ± 0.4
t_{max} (h)		2–8	8	4–8
Plasma AUC_{0-24} (h*μg/ml)	i.v., 5 mg/kg	32.8 ± 2.2	40.1 ± 3.5 ++	45.2 ± 2.5 ***
Fold change AUC_{0-24}		1	1.2	1.4

Data are given as mean ± S.D. (n = 4–6). C_{max}, maximum concentration in plasma; t_{max}, time point (h) of maximum plasma concentration (range for individual mice). *, $P < 0.05$; **, $P < 0.01$; ***, $P < 0.001$ compared to WT mice. +, $P < 0.05$; ++, $P < 0.01$; +++, $P < 0.001$ compared to Cyp3aXAV mice.

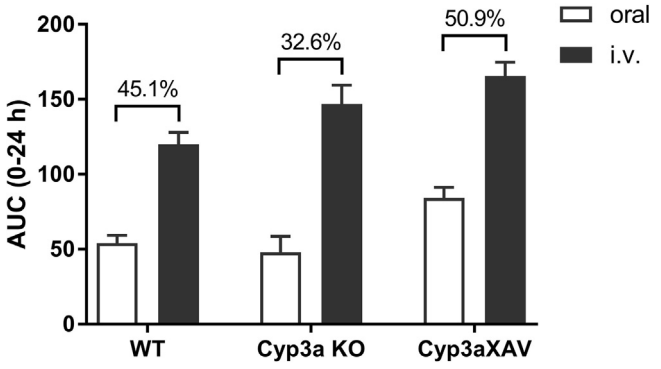

Fig. 5. Oral and intravenous plasma AUC and oral bioavailability of quizartinib in female WT, Cyp3a KO and Cyp3aXAV mice over 24 h (n = 4–6). Percentage values indicate $AUC_{oral}/AUC_{i.v.}$ for each strain. The dose-normalized oral and i.v. plasma AUC_{0-24} was used.

secondary changes in the hABCB1- and hABCG2-overexpressing K562 cells contributed to their increased sensitivity to quizartinib. Nonetheless, there can be little doubt that *in vivo* quizartinib is significantly transported by mAbcb1 and mAbcg2. The demonstration that quizartinib can directly interact with hABCB1 and hABCG2 through a number of assays including inhibition of transport of other drugs, and inhibition of photolabeling by a specific radioactive ligand of the

transport proteins (Li et al., 2017; Bhullar et al., 2013) is in line with this, and suggests that these interactions occurred through competitive inhibition by transported quizartinib.

Looking at the collective data, one has to consider the possibility that ABCB1 and perhaps ABCG2 expression in AML cells may directly contribute to some level of resistance to quizartinib therapy, in which case it could be worthwhile to try and inhibit these transporters. Although Marzac et al. found that 22 out of 26 (85%) patients with AML and FLT3-ITD did not express a functional ABCB1 (Marzac et al., 2006), such patients do not appear to have significantly reduced ABCG2 mRNA (Schaich et al., 2005; Nasilowska-Adamska et al., 2014). It will therefore be of interest to assess what fraction of FLT3-ITD AML patients might benefit from such an approach. Moreover, while CNS involvement is uncommon in AML among adults, in infants it is more frequent, and in such cases one could consider improving the CNS distribution of quizartinib using effective ABCB1 and ABCG2 inhibitors like elacridar, as previously demonstrated in mice for sunitinib (Tang et al., 2012a). In this respect it is worth noting that deficiency of mAbcb1 and mAbcg2 in mice resulted in quizartinib brain-to-plasma ratios of 1.1 (i.e., 110%), indicating a relatively good penetration of this drug into the brain once the BBB ABC efflux transporters were inactive.

There is very little publicly available information on the possible interaction of quizartinib with CYP3A, either *in vitro* or *in vivo*. In our 8 and 24 h oral experiments in Cyp3a knockout and Cyp3aXAV mice, we found there is some, most likely indirect, impact of mCyp3a and hCYP3A on the plasma levels and elimination of quizartinib in mice, with otherwise no significant effects on relative tissue distribution of the drug (Supplemental Figs. 3 and 4). The plasma AUC in Cyp3a knockout mice was not significantly altered compared to WT mice in either the 8 h or 24 h oral experiment (Fig. 4; Tables 1 and 2) or in the 24 h i.v. experiment (Supplemental Fig. 2; Table 2). However, in all tested conditions (oral 8 and 24 h, i.v. 8 h) the terminal elimination of quizartinib appeared to be significantly slower in the Cyp3a knockout mice (Fig. 4 and Supplemental Fig. 2), perhaps suggesting a limited role of mouse Cyp3a in the late elimination of quizartinib. Counter-intuitively, the plasma AUC was increased in Cyp3aXAV mice compared to WT mice in the 8 h oral experiment (not significant, Table 1), 24 h oral experiment ($P < 0.001$, Table 2), and i.v. 24 h experiment ($P < 0.001$, Table 2). They were also increased relative to the *Cyp3a*$^{-/-}$ mice. This suggests that human CYP3A4 does not have a strong direct impact in reducing systemic availability of quizartinib, because then a decrease in plasma AUC would have been expected.

Collectively, these results suggest that loss of Cyp3a or over-expression of human CYP3A4 did not directly result in the predicted increase or decrease, respectively, of quizartinib availability in the case that CYP3A would be a dominant player in metabolizing quizartinib in mice. Rather, the data suggest that there is a secondary, perhaps compensatory, modulation of one or more other, as yet unidentified, quizartinib uptake or detoxification systems when CYP3A is removed or reintroduced, which is/are responsible for the modest pharmacokinetic changes that we observed between the strains. As explained above, we have observed similar compensatory phenomena for the metabolism of midazolam by Cyp3a in Cyp3a knockout mice (van Waterschoot et al., 2008; van Waterschoot et al., 2009). Nonetheless, the most likely interpretation therefore is that CYP3A itself is not an important determinant of quizartinib pharmacokinetics in mice, but its absence or presence does affect activity of one or more other quizartinib detoxification systems. It is worth noting that we cannot exclude that, for instance, mouse Cyp2c enzymes, which are upregulated in *Cyp3a*$^{-/-}$ mice (van Waterschoot et al., 2008) may also metabolize quizartinib, thus potentially masking a more pronounced impact of CYP3A on quizartinib pharmacokinetics than suggested by our *in vivo* experiments.

In accordance with a limited direct impact of mCyp3a and human CYP3A4 on quizartinib metabolism in mice, we did not observe marked changes in absolute oral bioavailability between wild-type (45.1%), *Cyp3a*$^{-/-}$ (32.6%), and Cyp3aXAV (50.9%) mice (Fig. 5). Interestingly, although the uptake rate of quizartinib after oral administration (for mice) is not very fast (t_{max} between 2 and 8 h), the oral availability is still fair.

5. Conclusion

To the best of our knowledge, our study is the first to show that quizartinib can be transported by hABCB1, mAbcb1 and mAbcg2, and that the brain penetration of quizartinib, but not its oral availability, can be markedly limited by both mAbcb1 and mAbcg2. This could mean that it may be worthwhile to inhibit ABCB1 and ABCG2 with a pharmacological inhibitor when treating malignant lesions present in part or in whole behind the blood-brain barrier with quizartinib. Our *in vivo* experiments do not point to a prominent role of CYP3A in limiting the oral availability or tissue distribution of quizartinib, at least in mice, but we cannot exclude that there are significant changes in other quizartinib-detoxifying systems. Finally, the oral bioavailability of quizartinib in mice is quite high, in spite of a modest rate of net absorption. If this also applies in humans this could mean that there is a reduced risk of high CYP3A-related variation in exposure of this drug.

Acknowledgements

This work was supported in part by fellowships from the China Scholarship Council (to C.G. and W.L.) and internal funds from the Netherlands Cancer Institute.

Appendix A. Supplementary data

Supplementary data to this article can be found online at https://doi.org/10.1016/j.ijpharm.2018.12.014.

References

Baker, S.D., Zimmerman, E.I., Wang, Y.-D., Orwick, S., Zatechka, D.S., Buaboonnam, J., Neale, G.A., Olsen, S.R., Enemark, E.J., Shurtleff, S., 2013. Emergence of polyclonal FLT3 tyrosine kinase domain mutations during sequential therapy with sorafenib and sunitinib in FLT3-ITD–positive acute myeloid leukemia. Clin. Cancer Res. 19, 5758–5768.

Benderra, Z., Faussat, A.M., Sayada, L., Perrot, J.-Y., Tang, R., Chaoui, D., Morjani, H., Marzac, C., Marie, J.-P., Legrand, O., 2005. MRP3, BCRP, and P-glycoprotein activities are prognostic factors in adult acute myeloid leukemia. Clin. Cancer Res. 11, 7764–7772.

Bhullar, J., Natarajan, K., Shukla, S., Mathias, T.J., Sadowska, M., Ambudkar, S.V., Baer, M.R., 2013. The FLT3 inhibitor quizartinib inhibits ABCG2 at pharmacologically relevant concentrations, with implications for both chemosensitization and adverse drug interactions. PLoS One 8, e71266.

Borst, P., Elferink, R.O., 2002. Mammalian ABC transporters in health and disease. Annu. Rev. Biochem. 71, 537–592.

Chao, Q., Sprankle, K.G., Grotzfeld, R.M., Lai, A.G., Carter, T.A., Velasco, A.M., Gunawardane, R.N., Cramer, M.D., Gardner, M.F., James, J., 2009. Identification of N-(5-tert-butyl-isoxazol-3-yl)-N′-{4-[7-(2-morpholin-4-yl-ethoxy) imidazo [2, 1-b][1, 3] benzothiazol-2-yl] phenyl} urea dihydrochloride (AC220), a uniquely potent, selective, and efficacious FMS-like tyrosine kinase-3 (FLT3) inhibitor. J. Med. Chem. 52, 7808–7816.

Chevallier, P., Labopin, M., Turlure, P., Prebet, T., Pigneux, A., Hunault, M., Filanovsky, K., Cornillet-Lefebvre, P., Luquet, I., Lode, L., 2011. A new Leukemia Prognostic Scoring System for refractory/relapsed adult acute myelogeneous leukaemia patients: a GOELAMS study. Leukemia 25, 939–944.

Cortes, J.E., Kantarjian, H., Foran, J.M., Ghirdaladze, D., Zodelava, M., Borthakur, G., Gammon, G., Trone, D., Armstrong, R.C., James, J., 2013. Phase I study of quizartinib administered daily to patients with relapsed or refractory acute myeloid leukemia irrespective of FMS-like tyrosine kinase 3–internal tandem duplication status. J. Clin. Oncol. 31, 3681–3687.

Döhner, H., Weisdorf, D.J., Bloomfield, C.D., 2015. Acute myeloid leukemia. N. Engl. J. Med. 373, 1136–1152.

Durmus, S., Sparidans, R.W., Wagenaar, E., Beijnen, J.H., Schinkel, A.H., 2012. Oral availability and brain penetration of the B-RAFV600E inhibitor vemurafenib can be enhanced by the P-GLYCOprotein (ABCB1) and breast cancer resistance protein (ABCG2) inhibitor elacridar. Mol. Pharm. 9, 3236–3245.

Fiedler, W., Kayser, S., Kebenko, M., Janning, M., Krauter, J., Schittenhelm, M., Götze, K., Weber, D., Göhring, G., Teleanu, V., 2015. A phase I/II study of sunitinib and intensive chemotherapy in patients over 60 years of age with acute myeloid leukaemia and activating FLT3 mutations. Br. J. Haematol. 169, 694–700.

Fleischmann, M., Schnetzke, U., Schrenk, K.G., Schmidt, V., Sayer, H.G., Hilgendorf, I., Hochhaus, A., Scholl, S., 2017. Outcome of FLT3-ITD-positive acute myeloid leukemia: impact of allogeneic stem cell transplantation and tyrosine kinase inhibitor treatment. J. Cancer Res. Clin. Oncol. 143, 337–345.
Gilliland, D.G., Griffin, J.D., 2002. The roles of FLT3 in hematopoiesis and leukemia. Blood 100, 1532–1542.
Guengerich, F.P., 1995. Human cytochrome P450 enzymes. In: *Cytochrome P450*. Springer, pp. 473–535.
Jonker, J.W., Buitelaar, M., Wagenaar, E., Van Der Valk, M.A., Scheffer, G.L., Scheper, R.J., Plösch, T., Kuipers, F., Elferink, R.P.O., Rosing, H., 2002. The breast cancer resistance protein protects against a major chlorophyll-derived dietary phototoxin and protoporphyria. Proc. Natl. Acad. Sci. 99, 15649–15654.
Jonker, J.W., Freeman, J., Bolscher, E., Musters, S., Alvi, A.J., Titley, I., Schinkel, A.H., Dale, T.C., 2005. Contribution of the ABC transporters Bcrp1 and Mdr1a/1b to the side population phenotype in mammary gland and bone marrow of mice. Stem Cells 23, 1059–1065.
Kampa-Schittenhelm, K.M., Heinrich, M.C., Akmut, F., Döhner, H., Döhner, K., Schittenhelm, M.M., 2013. Quizartinib (AC220) is a potent second generation class III tyrosine kinase inhibitor that displays a distinct inhibition profile against mutant-FLT3,-PDGFRA and-KIT isoforms. Mol. Cancer 12, 19.
Kindler, T., Lipka, D.B., Fischer, T., 2010. FLT3 as a therapeutic target in AML: still challenging after all these years. Blood 116, 5089–5102.
Kottaridis, P.D., Gale, R.E., Frew, M.E., Harrison, G., Langabeer, S.E., Belton, A.A., Walker, H., Wheatley, K., Bowen, D.T., Burnett, A.K., 2001. The presence of a FLT3 internal tandem duplication in patients with acute myeloid leukemia (AML) adds important prognostic information to cytogenetic risk group and response to the first cycle of chemotherapy: analysis of 854 patients from the United Kingdom Medical Research Council AML 10 and 12 trials. Blood 98, 1752–1759.
Lagas, J.S., van Waterschoot, R.A., Sparidans, R.W., Wagenaar, E., Beijnen, J.H., Schinkel, A.H., 2010. Breast cancer resistance protein and P-glycoprotein limit sorafenib brain accumulation. Mol. Cancer Ther. 9, 319–326.
Levis, M., Small, D., 2005. FLT3 tyrosine kinase inhibitors. Int. J. Hematol. 82, 100–107.
Li, J., Kumar, P., Anreddy, N., Zhang, Y.-K., Wang, Y.-J., Chen, Y., Talele, T.T., Gupta, K., Trombetta, L.D., Chen, Z.-S., 2017. Quizartinib (AC220) reverses ABCG2-mediated multidrug resistance: In vitro and in vivo studies. Oncotarget 8, 93785–93799.
Marzac, C., Teyssandier, I., Perrot, J.-Y., Faussat, A.-M., Tang, R., Casadevall, N., Marie, J.-P., Legrand, O., 2006. Flt3 internal tandem duplication and P-glycoprotein functionality in 171 patients with acute myeloid leukemia. Clin. Cancer Res. 12, 7018–7024.
Meshinchi, S., Appelbaum, F.R., 2009. Structural and functional alterations of FLT3 in acute myeloid leukemia. Clin. Cancer Res. 15, 4263–4269.
Nasilowska-Adamska, B., Solarska, I., Paluszewska, M., Malinowska, I., Jedrzejczak, W.W., Warzocha, K., 2014. FLT3-ITD and MLL-PTD influence the expression of MDR-1, MRP-1, and BCRP mRNA but not LRP mRNA assessed with RQ-PCR method in adult acute myeloid leukemia. Ann. Hematol. 93, 577–593.
Pluchino, K.M., Hall, M.D., Goldsborough, A.S., Callaghan, R., Gottesman, M.M., 2012. Collateral sensitivity as a strategy against cancer multidrug resistance. Drug Resist. Updates 15, 98–105.
Retmana, I.A., Wang, J., Schinkel, A.H., Schellens, J.H., Beijnen, J.H., Sparidans, R.W., 2017. Liquid chromatography-tandem mass spectrometric assay for the quantitative determination of the tyrosine kinase inhibitor quizartinib in mouse plasma using salting-out liquid-liquid extraction. J. Chromatogr. B 1061, 300–305.
Röllig, C., Müller-Tidow, C., Hüttmann, A., Noppeney, R., Kunzmann, V., Baldus, C.D., Brandts, C.H., Krämer, A., Schäfer-Eckart, K., Neubauer, A., 2014. Sorafenib versus placebo in addition to standard therapy in younger patients with newly diagnosed acute myeloid leukemia: results from 267 patients treated in the randomized placebo-controlled SAL-Soraml trial. Am Soc. Hematology.
Rowe, J.M., Tallman, M.S., 2010. How I treat acute myeloid leukemia. Blood 116, 3147–3156.
Sanga, M., James, J., Marini, J., Gammon, G., Hale, C., Li, J., 2017. An open-label, single-dose, phase 1 study of the absorption, metabolism and excretion of quizartinib, a highly selective and potent FLT3 tyrosine kinase inhibitor, in healthy male subjects, for the treatment of acute myeloid leukemia. Xenobiotica 47, 856–869.
Schaich, M., Soucek, S., Thiede, C., Ehninger, G., Illmer, T., 2005. MDR1 and MRP1 gene expression are independent predictors for treatment outcome in adult acute myeloid leukaemia. Br. J. Haematol. 128, 324–332.
Schinkel, A.H., Jonker, J.W., 2003. Mammalian drug efflux transporters of the ATP binding cassette (ABC) family: an overview. Adv. Drug Deliv. Rev. 55, 3–29.
Schinkel, A.H., Mayer, U., Wagenaar, E., Mol, C.A., Van Deemter, L., Smit, J.J., Van Der Valk, M.A., Voordouw, A.C., Spits, H., Van Tellingen, O., 1997. Normal viability and altered pharmacokinetics in mice lacking mdr1-type (drug-transporting) P-glycoproteins. Proc. Natl. Acad. Sci. 94, 4028–4033.
Schlenk, R., Frech, P., Weber, D., Brossart, P., Horst, H., Kraemer, D., Held, G., Ringhoffer, M., Burchardt, A., Kobbe, G., 2017. Impact of pretreatment characteristics and salvage strategy on outcome in patients with relapsed acute myeloid leukemia. Leukemia.
Schnittger, S., Schoch, C., Dugas, M., Kern, W., Staib, P., Wuchter, C., Löffler, H., Sauerland, C.M., Serve, H., Büchner, T., 2002. Analysis of FLT3 length mutations in 1003 patients with acute myeloid leukemia: correlation to cytogenetics, FAB subtype, and prognosis in the AMLCG study and usefulness as a marker for the detection of minimal residual disease. Blood 100, 59–66.
Serve, H., Krug, U., Wagner, R., Sauerland, M.C., Heinecke, A., Brunnberg, U., Schaich, M., Ottmann, O., Duyster, J., Wandt, H., 2013. Sorafenib in combination with intensive chemotherapy in elderly patients with acute myeloid leukemia: results from a randomized, placebo-controlled trial. J. Clin. Oncol. 31, 3110–3118.
Siegel, R.L., Miller, K.D., Jemal, A., 2017. Cancer statistics, 2017. CA Cancer J. Clin. 67, 7–30.
Tang, S.C., de Vries, N., Sparidans, R.W., Wagenaar, E., Beijnen, J.H., Schinkel, A.H., 2013. Impact of P-glycoprotein (ABCB1) and breast cancer resistance protein (ABCG2) gene dosage on plasma pharmacokinetics and brain accumulation of dasatinib, sorafenib, and sunitinib. J. Pharmacol. Exp. Ther. 346, 486–494.
Tang, S.C., Lagas, J.S., Lankheet, N.A., Poller, B., Hillebrand, M.J., Rosing, H., Beijnen, J.H., Schinkel, A.H., 2012a. Brain accumulation of sunitinib is restricted by P-glycoprotein (ABCB1) and breast cancer resistance protein (ABCG2) and can be enhanced by oral elacridar and sunitinib coadministration. Int. J. Cancer 130, 223–233.
Tang, S.C., Lankheet, N.A., Poller, B., Wagenaar, E., Beijnen, J.H., Schinkel, A.H., 2012b. P-glycoprotein (ABCB1) and breast cancer resistance protein (ABCG2) restrict brain accumulation of the active sunitinib metabolite N-desethyl sunitinib. J. Pharmacol. Exp. Ther. 341, 164–173.
Taylor, S.J., Duyvestyn, J.M., Dagger, S.A., Dishington, E.J., Rinaldi, C.A., Dovey, O.M., Vassiliou, G.S., Grove, C.S., Langdon, W.Y., 2017. Preventing chemotherapy-induced myelosuppression by repurposing the FLT3 inhibitor quizartinib. Sci. Transl. Med. 9, eaam8060.
Thiede, C., Steudel, C., Mohr, B., Schaich, M., Schäkel, U., Platzbecker, U., Wermke, M., Bornhäuser, M., Ritter, M., Neubauer, A., 2002. Analysis of FLT3-activating mutations in 979 patients with acute myelogenous leukemia: association with FAB subtypes and identification of subgroups with poor prognosis. Blood 99, 4326–4335.
van Herwaarden, A.E., Wagenaar, E., van der Kruijssen, C.M., van Waterschoot, R.A., Smit, J.W., Song, J.-Y., van der Valk, M.A., van Tellingen, O., van der Hoorn, J.W., Rosing, H., 2007. Knockout of cytochrome P450 3A yields new mouse models for understanding xenobiotic metabolism. J. Clin. Investig. 117, 3583–3592.
van Hoppe, S., Sparidans, R.W., Wagenaar, E., Beijnen, J.H., Schinkel, A.H., 2017. Breast cancer resistance protein (BCRP/ABCG2) and P-glycoprotein (P-gp/ABCB1) transport afatinib and restrict its oral availability and brain accumulation. Pharmacol. Res. 120, 43–50.
van Waterschoot, R.A., Rooswinkel, R.W., Wagenaar, E., van der Kruijssen, C.M., van Herwaarden, A.E., Schinkel, A.H., 2009. Intestinal cytochrome P450 3A plays an important role in the regulation of detoxifying systems in the liver. FASEB J. 23, 224–231.
van Waterschoot, R.A., van Herwaarden, A.E., Lagas, J.S., Sparidans, R.W., Wagenaar, E., van der Kruijssen, C.M., Goldstein, J.A., Zeldin, D.C., Beijnen, J.H., Schinkel, A.H., 2008. Midazolam metabolism in cytochrome P450 3A knockout mice can be attributed to up-regulated CYP2C enzymes. Mol. Pharmacol. 73, 1029–1036.
Vlaming, M.L., Lagas, J.S., Schinkel, A.H., 2009. Physiological and pharmacological roles of ABCG2 (BCRP): recent findings in Abcg2 knockout mice. Adv. Drug Deliv. Rev. 61, 14–25.
Wagner, K., Damm, F., Thol, F., Göhring, G., Görlich, K., Heuser, M., Schäfer, I., Schlegelberger, B., Heil, G., Ganser, A., 2011. FLT3-internal tandem duplication and age are the major prognostic factors in patients with relapsed acute myeloid leukemia with normal karyotype. Haematologica 96, 681–686.
Wattad, M., Weber, D., Döhner, K., Krauter, J., Gaidzik, V., Paschka, P., Heuser, M., Thol, F., Kindler, T., Lübbert, M., 2017. Impact of salvage regimens on response and overall survival in acute myeloid leukemia with induction failure. Leukemia 31, 1306–1313.
Zanger, U.M., Schwab, M., 2013. Cytochrome P450 enzymes in drug metabolism: regulation of gene expression, enzyme activities, and impact of genetic variation. Pharmacol. Ther. 138, 103–141.
Zarrinkar, P.P., Gunawardane, R.N., Cramer, M.D., Gardner, M.F., Brigham, D., Belli, B., Karaman, M.W., Pratz, K.W., Pallares, G., Chao, Q., 2009. AC220 is a uniquely potent and selective inhibitor of FLT3 for the treatment of acute myeloid leukemia (AML). Blood 114, 2984–2992.
Zhang, Y., Huo, M., Zhou, J., Xie, S., 2010. PKSolver: An add-in program for pharmacokinetic and pharmacodynamic data analysis in Microsoft Excel. Comput. Methods Programs Biomed. 99, 306–314.